FARADAY

Oxyhalogen–sulfur chemistry: Non-linear oxidation of 2-aminoethanethiolsulfuric acid (AETSA) by bromate in acidic medium†

James Darkwa,[a] Claudius Mundoma[b] and Reuben H. Simoyi*[b]

[a] *Department of Chemistry, University of the North, Private Bag X1106, Sovenga 0727, South Africa*

[b] *Department of Chemistry, West Virginia University, Morgantown, WV 26506-6045, USA*

The reaction between bromate and 2-aminoethanethiolsulfuric acid, $H_2NCH_2CH_2S{-}SO_3H$ (AETSA), has been studied in high acid environments. The stoichiometry in excess AETSA is $BrO_3^- + H_2NCH_2CH_2S{-}SO_3H + H_2O \rightarrow H_2NCH_2CH_2SO_3H + SO_4^{2-} + 2H^+ + Br^-$. In excess BrO_3^- the stoichiometry is: $7BrO_3^- + 5H_2NCH_2CH_2S{-}SO_3H \rightarrow 5Br(H)NCH_2CH_2SO_3H + 5SO_4^{2-} + Br_2 + 3H^+ + H_2O$. The reaction displays clock reaction characteristics in which there is initial quiescence followed by a sudden and rapid formation of Br_2(aq). The oxidation proceeds by successive addition of oxygen on the inner sulfur atom followed by cleavage of the S—S bond to form taurine and SO_4^{2-}. The Br_2(aq) and the HOBr in solution oxidize the taurine to form a mixture of monobromotaurine and dibromotaurine. Computer simulations of a proposed 13-step reaction scheme produced a reasonable fit to the experimental data.

The use of oxyhalogen ions IO_3^-, BrO_3^- and ClO_2^- as oxidants invariably produces non-linear kinetics characterized by such features as autocatalysis, autoinhibition and clocking.[1–3] Overall, we have a full grasp of the causes of these non-linearities. Hence, the cornerstone of non-linear dynamics in chemistry over the years has been oxyhalogen chemistry.[5] The Belousov–Zhabotinsky[5] reaction for example, has been exhaustively studied and there is rationalization of global behaviour from single-step reaction mechanisms.[6]

We now know that reactions of sulfur compounds, especially the S^{2-}, HS^- and small water-soluble organic molecules can generate the same non-linearities as oxyhalogen compounds.[7–10] To date, there are several chemical systems involving sulfur compounds which show clock reaction characteristics, autocatalysis, autoinhibition, travelling waves and spatiotemporal patterns.[11–14] It is generally conjectured that the sulfur centre' s propensity to polymerize represents an in-built non-linearity in the global dynamics of reactions that involve sulfur compounds. We do not know as much about the reactivity of the sulfur centre as we do for oxyhalogens. In order to understand the origin of the non-linearities observed with sulfur compounds, we started a series of studies whose primary aim is to systematically investigate, and hopefully deduce, a generalized algorithm for the oxidation of the sulfur centre.[15] The use of small organic sulfur compounds helps to limit the degree of sulfur–sulfur polymerizations to no more than the dimeric species from pure steric considerations. In general, our series of studies show that the oxidation of the sulfur centre in aqueous environments involves successive addition of oxygen onto the sulfur centre up to the sulfonic acid stage, RSO_3H, before cleavage of the C—S bond to form sulfate.[16] A number of observations, however, are still unexplained. There has been no quantification of free radical formation, for example, and the cleavage of the S—S bond after it has been formed has not been characterized. The sulfonic acid, for instance is considered to be quite stable, and that cleavage of the C—S bond may require very strong oxidizing agents to effect.[16]

In some of our recent work, we studied the oxidation of 2-aminoethanethiolsulfuric acid by iodate in acidic medium.[17] Our motivation for this study was the need to deduce the conditions under which the S—S bond and the C—S bond in the thiolsulfuric acid cleaved, as well as to determine the reaction products. The reaction of IO_3^- and AETSA presented some very complex global reaction dynamics which included clock reaction characteristics and the transient formation of an intermediate, I_2/I_3^-, which could be easily detected by its spectrum and absorption peaks at 286 and 353 nm.[17] Derivation of the kinetics rate law for the reaction was complicated by the fact that in medium to high acid concentrations, the Dushman reaction:[18]

$$IO_3^- + 5I^- + 6H^+ \rightarrow 3I_2 + 3H_2O \qquad (1)$$

was fast enough to produce I_2 at a rate faster than I_2 could oxidize the substrate. Hence production of I_2 did not indicate that all the substrate had been oxidized. The stoichiometry of the reaction was also mixed, without quantitative formation of SO_4^{2-} (approximately only one of the S atoms was oxidized to SO_4^{2-}).

In this paper we report on the oxidation of AETSA by acidic bromate. A comparison of the BrO_3^-–AETSA reaction with the IO_3^-–AETSA reaction can give a better insight into the oxidation of AETSA, as well as the reaction products. Our preliminary experiments had shown that the reaction of Br_2(aq) with AETSA was significantly faster than the corresponding I_2(aq)–AETSA reaction and that it was essentially complete within a fraction of a second. We thus anticipated much simpler kinetics since the reaction:[19]

$$BrO_3^- + 5Br^- + 6H^+ \rightarrow 3Br_2(aq) + 3H_2O \qquad (2)$$

could only produce long-lived aqueous Br_2 after the AETSA had been totally consumed.

† Part 21 in the series: Non-linear dynamics in chemistry derived from sulfur chemistry. Part 20: B. S. Martincigh, C. R. Chinake and R. H. Simoyi, *Phys. Lett.*, submitted.

Experimental

Materials

Doubly distilled deionized water was used for the preparation of all stock solutions and their subsequent dilutions. ACS reagent grade $NaClO_4$ (Fisher) purified previously, was used for ionic strength adjustment for the reaction involving bromine and aminoethanethiolsulfuric acid. The following reagents were used without further purification: perchloric acid, 72%, sodium bromide and sodium bromate (Fisher); bromine, aminoethanethiolsulfuric acid (Aldrich). $HClO_4$ was standardized against sodium hydroxide using methyl orange as the indicator. All photosensitive solutions were stored in a dark place when not in use or protected from light by covering them with aluminum foil. Bromine solution was kept in a sealed container, in the refrigerator, because of its high volatility. Deuterium oxide was used for ^1H NMR studies on the products and parent compounds.

Methods

Two systems were studied, namely the BrO_3^-–AETSA reaction and the Br_2–AETSA reaction. Both systems were run on a Hi-Tech Scientific SF-61AF stopped-flow spectrophotometer with an M300 monochromator and a spectrascan control unit. Digitization and amplifying of signals was done *via* an Omega Engineering DAS-50/1 16-bit A/D board interfaced with a Tandon computer for data storage and analysis. Reaction progress was followed by monitoring the evolution of Br_2 at 390 nm where it has an absorption peak for which we deduced an absorptivity coefficient of 142 M^{-1} cm^{-1}. All concentrations reported are post-mixing and reactions were performed at 25 ± 0.1 °C.

Stoichiometric studies were done on a Perkin-Elmer Lambda 2S UV–VIS Spectrophotometer and identification of the organic product was done on a JEOL-270 MHz NMR spectrometer. Qualitative analysis of sulfate was done by precipitating it as $BaSO_4$. Quantification was difficult due to interference from the bromate ion which forms a precipitate of $Ba(BrO_3)_2$ with $BaCl_2$ in conditions of high ionic strength. The amount of bromine produced or consumed was quantified spectrophotometrically by measuring its absorbance at 390 nm. Solutions of varying ratios of oxidant to reductant were incubated for periods of at least 24 h before they were used for any stoichiometric determinations.

Results

Stoichiometry

The stoichiometry of the reaction was very complex and was strictly dependent on the initial concentration ratios of the oxidant, BrO_3^-, to reductant, AETSA. In excess AETSA conditions the stoichiometry was deduced as:

$$BrO_3^- + H_2NCH_2CH_2S{-}SO_3H + H_2O \rightarrow H_2NCH_2CH_2SO_3H + SO_4^{2-} + 2H^+ + Br^- \quad (3)$$

The major product, $H_2NCH_2CH_2SO_3H$ (taurine), was identified by its UV and NMR spectra.[20] The proton NMR spectrum of taurine is quite distinct with two triplets which show up at $\delta_\alpha = 2.56$–2.64 and $\delta_\beta = 2.74$–2.81 in neutral conditions. These triplets are slightly shifted downfield in acidic medium due to the protonation of the amino group:

$$\overset{\beta}{H_2N}{-}\overset{\alpha}{CH_2}{-}CH_2{-}SO_3H + H^+ \rightleftharpoons \overset{+}{H_3N}{-}\overset{\beta}{CH_2}{-}\overset{\alpha}{CH_2}{-}SO_3H$$

Due to the rapid exchange with solvent, the protons on the nitrogen and the one on the sulfonic acid group cannot be detected.

In excess AETSA conditions the NMR spectrum shows a combination of the original AETSA multiplet peak (centred *ca.* $\delta = 3.27$) and the two new taurine triplets. Successive addition of BrO_3^- past the stoichiometric point will eventually lead to the disappearance of the AETSA peak. The AETSA peak disappears just before the stoichiometric equivalent has been reached because the NMR technique is sensitive only to *ca.* 5%.

Excess BrO_3^- was determined iodometrically.[19,21] In excess BrO_3^-, two more reactions became important: the formation of Br_2(aq) from excess BrO_3^- [reaction (2)] and the bromination of the taurine produced in reaction (3) to form bromotaurine:

$$Br_2(aq) + H_2NCH_2CH_2SO_3H \rightarrow Br(H)NCH_2CH_2SO_3H + Br^- + H^+ \quad (4)$$

The bromotaurine was identified by the downfield shift of the two taurine triplets ($\Delta\delta \approx 0.2$ from taurine peaks) as well as the IR spectrum. The stoichiometry was not quantitative as the bromotaurine in reaction (4) is known to disproportionate to taurine and dibromotaurine:[22]

$$2Br(H)NCH_2CH_2SO_3H \rightleftharpoons H_2NCH_2CH_2SO_3H + Br_2NCH_2CH_2SO_3H \quad (5)$$

Reaction (5) gives an equilibrium mixture of taurine, mono- and di-bromotaurine.

Thus, the overall stoichiometry deduced in excess BrO_3^- was

$$7BrO_3^- + 5H_2NCH_2CH_2S{-}SO_3H \rightarrow 5Br(H)NCH_2CH_2SO_3H + 5SO_4^{2-} + Br_2 + 3H^+ + H_2O \quad (6)$$

Slightly more than 7 mol of BrO_3^- to 5 mol of AETSA were used as the monobromotaurine disproportionated according to reaction (5).

A direct stoichiometric determination was made of the Br_2–AETSA reaction. The determination was performed by a combination of iodometric and spectroscopic techniques. For iodometric techniques, the concentration of AETSA was increased successively at constant [Br_2(aq)]. The stoichiometry was determined as the point where the Br_2(aq) just vanished.

AETSA has strong absorption peaks at 240 and 214 nm. Addition of Br_2 gave no noticeable change in the 240 nm peak, although the 214 nm peak decreased. Excess Br_2 was detected by the rise of a peak at 390 nm, as well as another peak at 266 nm. The peak at 390 nm was so far removed from the AETSA peaks that quantitative Br_2(aq) determination could be effected. The ratio of Br_2(aq) to AETSA was slightly less than 4, suggesting the following stoichiometry:

$$4Br_2(aq) + H_2NCH_2CH_2S{-}SO_3H + 4H_2O \rightarrow Br(H)NCH_2CH_2SO_3H + SO_4^{2-} + 9H^+ + 7Br^- \quad (7)$$

The equilibrium represented by reaction (5) also produced some dibromotaurine which distorted the stoichiometry. Dibromotaurine has a very strong absorption peak at 240 nm[22] which can explain the lack of spectral activity at 240 nm upon addition of Br_2(aq). It also has a weak absorption peak at 336 nm. Monobromotaurine, on the other hand, has a very weak absorption at 280 nm, and will be swamped even by very low concentrations of the dibromotaurine. The monobromotaurine can be observed spectrally only at low Br_2 concentrations.

Br_2–taurine reaction. For comparison, the pure reaction of Br_2(aq) and taurine was also studied. Taurine almost instantly decolorizes bromine until the stoichiometric equivalent is

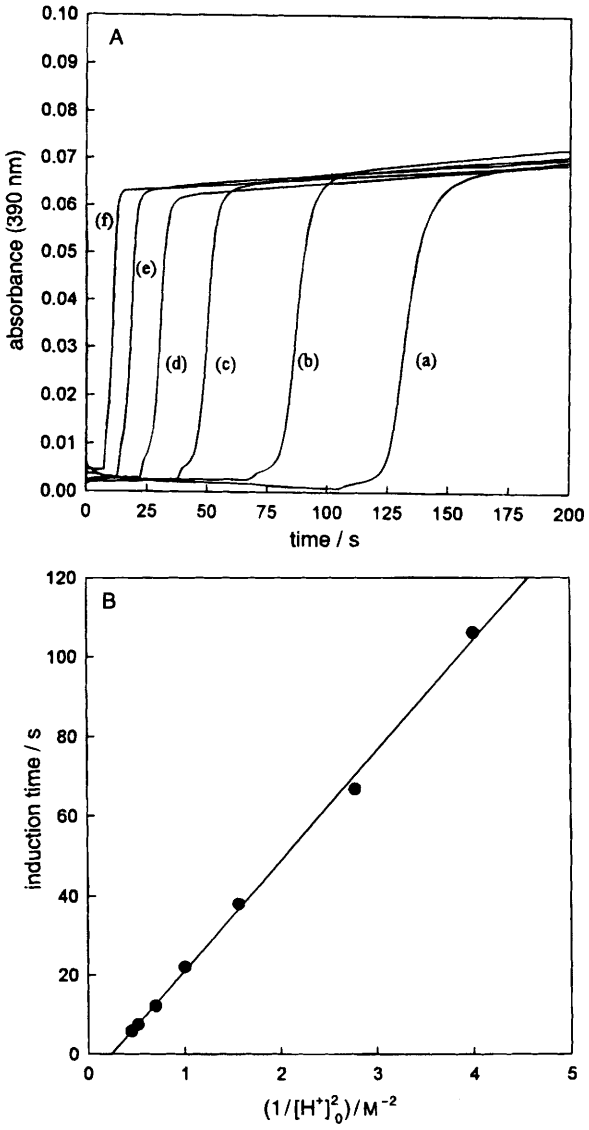

Fig. 1 (A) Absorbance traces at $\lambda = 390$ nm in excess BrO_3^- over AETSA at varying initial acid concentrations. $[AETSA]_0 = 0.002$ M, $[BrO_3^-]_0 = 0.050$ M. $[H^+]_0 =$ (a) 0.50 M; (b) 0.60 M; (c) 0.80 M; (d) 1.0 M; (e) 1.20 M; (f) 1.40 M. (B) Acid dependence of the induction period from the data in Fig. 1(A).

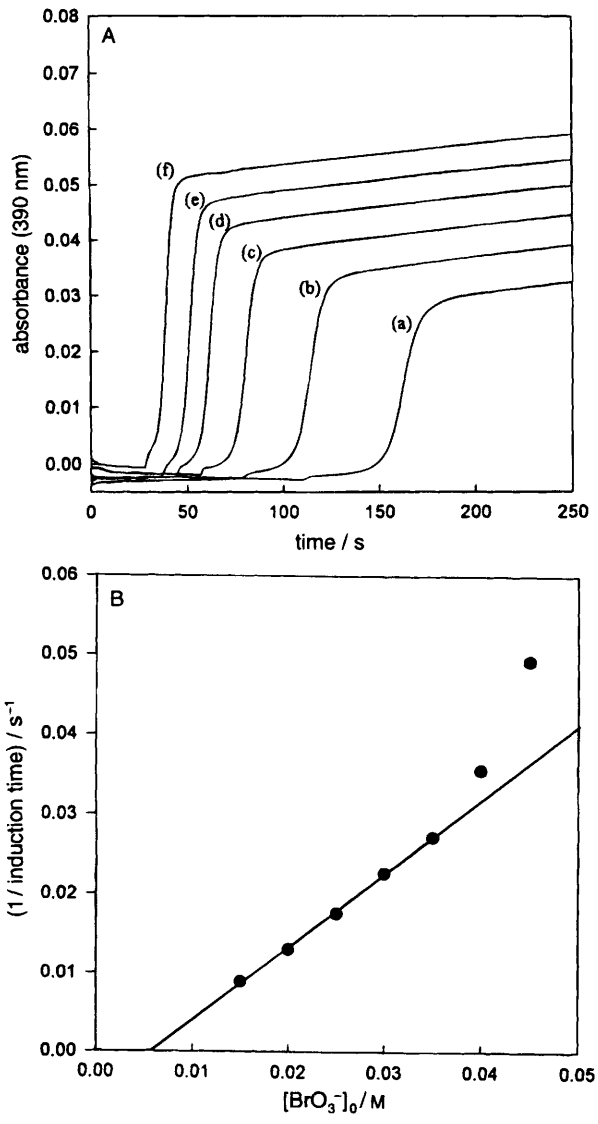

Fig. 2 (A) Absorbance traces at $\lambda = 390$ nm in excess BrO_3^- over AETSA at varying initial BrO_3^- concentrations. Note the 'kink' just after the end of the induction period. Higher BrO_3^- concentrations also increase the rate of formation of Br_2(aq). All the traces shown, (a)–(f), ultimately give the same final Br_2(aq) concentration. $[AETSA]_0 = 0.002$ M; $[H^+]_0 = 1.00$ M. $[BrO_3^-]_0 =$ (a) 0.015 M; (b) 0.020 M; (c) 0.025 M; (d) 0.030 M; (e) 0.035 M; (f) 0.040 M. (B) Plot of the inverse of the induction time against $[BrO_3^-]_0$. Linearity is lost at high bromate concentrations. $[AETSA]_0 = 0.002$ M; $[H^+]_0 = 1.0$ M

reached. The important facts from this experiment were:

(*a*) The C—S bond is not cleaved as no SO_4^{2-} is detected in the reaction product solution; (*b*) The reaction is very fast; (*c*) Bromine attacks the nitrogen end of the taurine to form mono- and di-bromotaurine. Both proton and ^{13}C NMR spectral data confirmed that the methylene groups $-CH_2-CH_2-$ were left unchanged by the oxidation of taurine by Br_2(aq).

Reaction characteristics (BrO_3^-–AETSA reaction):

The reaction dynamics are very complex. No noticeable activity could be observed in the reaction parameters in excess reductant (AETSA). Thus there was no change observed in the redox potential (platinum with a calomel reference), the specific bromide electrode, or absorbance at all the expected peaks (*e.g.* at the bromine peak at $\lambda = 390$ nm). All data reported here were in excess BrO_3^-(aq) and high acid strengths (pH $\leqslant 2$).

In general, the reaction displayed typical clock reaction characteristics in which there is reaction quiescence followed by a rapid change in absorptivity ($\lambda = 390$ nm) and redox potential at the end of the induction period. The formation of Br_2 seemed to occur in two distinct stages. After the initial Br_2(aq) formation, there is a noticeable 'kink' in the absorption-time trace after *ca.* 5–10 s (see Fig. 1A).

Acid dependence. Acid has a very strong catalytic effect on the reaction. Acid does not appear as a reactant, however, in the reaction stoichiometries (3), (6) and (7). Increase in acid concentration at constant $[BrO_3^-]_0/[AETSA]_0$ leads to much shorter induction times (see Fig. 1A). Induction time in this case is defined as the time lapse between mixing of the reagents and formation of Br_2(aq) and/or the rapid increase in redox potential. A plot of induction time *vs.* $[H^+]^{-2}$ gives a straight line with an intercept indistinguishable kinetically, from zero (see Fig. 1B). Acid concentrations affected the rate but not the final quantity of bromine obtained, nor any other stoichiometric constant.

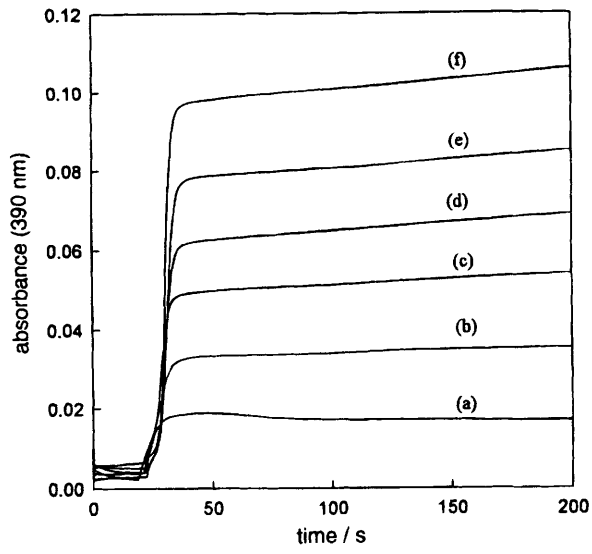

Fig. 3 Effect of varying $[AETSA]_0$ in excess $[BrO_3^-]_0$ conditions. The final $Br_2(aq)$ increases with $[AETSA]_0$, but the induction period does not change. $[BrO_3^-] = 0.050$ M; $[H^+] = 1.00$ M. [AETSA] = (a) 0.005 M; (b) 0.008 M; (c) 0.015 M; (d) 0.020 M; (e) 0.025 M; (f) 0.030 M.

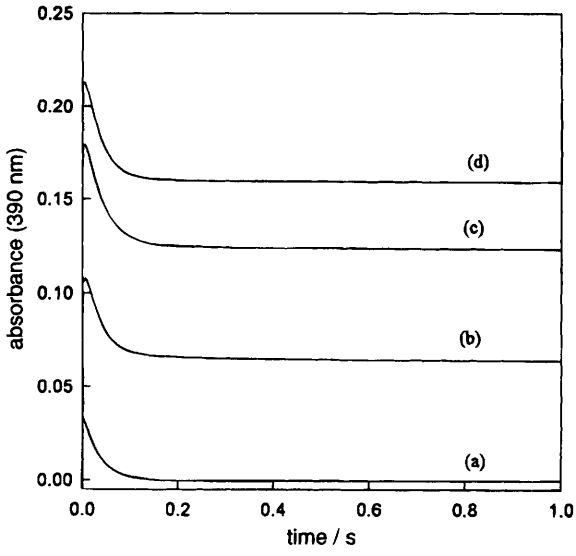

Fig. 5 Direct reaction of $Br_2(aq)$ and AETSA showing that the reaction is essentially complete within a fraction of a second. The stoichiometry of the reaction could also be deduced from these experiments. [AETSA] = 0.0005 M. $[Br_2(aq)]_0$ = (a) 0.0019 M; (b) 0.0027 M; (c) 0.0031 M; (d) 0.0038 M

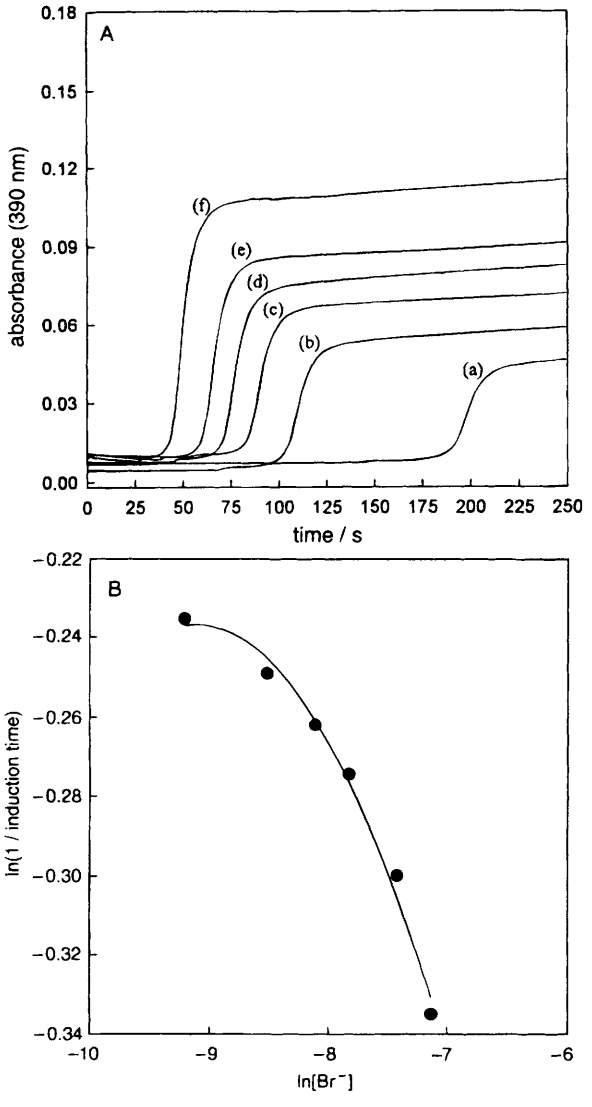

Fig. 4 (A) The catalytic effect of bromide: higher $[Br^-]_0$ decreases the length of the induction period and also increases the amount of $Br_2(aq)$ formed. $[AETSA]_0 = 0.002$ M; $[H^+]_0 = 0.80$ M $[BrO_3^+]_0 = 0.050$ M. $[Br^-]_0$ = (a) 0.00 M. (b) 0.0001 M; (c) 0.0002 M; (d) 0.0003 M; (e) 0.0004 M; (f) 0.0006 M. (B) Plot of inverse of induction time *vs.* the initial $[Br^-]_0$. Linearity is also maintained only at very low bromide concentrations.

Bromate dependence. Bromate also shortened the induction period, but not as strongly as the acid. BrO_3^-, however, strongly influences the rate of formation of $Br_2(aq)$ after the induction period (Fig. 2A). Reactions run in high BrO_3^- concentrations quickly attained the stoichiometric Br_2 concentrations as determined by reaction stoichiometry (6). The plot of $[BrO_3^-]_0$ *vs.* the inverse of the induction time is linear only in the limit of low $[BrO_3^-]_0$. At higher $[BrO_3^-]_0$ there is an anomalous increase in the rate of reaction (denoted by a rapid decrease in induction period). This data is shown in Fig. 2B.

AETSA variations. As long as the $[BrO_3^-]_0/[AETSA]_0$ ratio is high, AETSA concentrations did not affect the induction period (see Fig. 3). AETSA concentrations did, however, affect: (*a*) the rate of formation of $Br_2(aq)$ and (b) the amount of $Br_2(aq)$ formed.

The last observation is in line with the observed stoichiometry of reaction (6) in which amount of $Br_2(aq)$ is determined by the initial AETSA concentration.

Effect of bromide. Bromide also has a very strong catalytic effect on the reaction. Addition of small amounts of Br^- such that $[BrO_3^-]_0/[Br^-]_0 > 50$ significantly reduced the induction period (Fig. 4A). Br^- also increased both the final $Br_2(aq)$ concentration obtained as well as the rate of formation of $Br_2(aq)$ after the induction period. A plot of the inverse of the induction time *vs.* $[Br^-]_0$ gave a straight line at low $[Br^-]_0$ concentrations (Fig. 4B). The rate of reaction (deduced from the induction time), increased at a much faster rate in high $[Br^-]$ as the plot lost its linearity. The kink just after the end of the induction period was more pronounced at high $[Br^-]_0$.

The Br_2–AETSA reaction. The Br_2–AETSA reaction's relative rate is very important in determining the expected global reaction dynamics with respect to bromine production and the induction period. The reaction was extremely fast, often complete in less than 0.05 s, which is close to the limit of our stopped-flow ensemble. Fig. 5 shows some of the stopped-flow data for the Br_2–AETSA reaction. Fig. 5 also shows that the stopped-flow only catches the last one-third of the reaction [from calculating the expected initial $Br_2(aq)$ absorbance and comparing with the experimentally-determined initial absorbance of $Br_2(aq)$].

Mechanism

Reduction of BrO_3^-

The first step in BrO_3^- oxidations is the formation of reactive intermediates. BrO_3^- itself is very stable and thus a poor oxidizer. The lower oxidation states of bromine, +1, +3 and +4 are more powerful oxidizing agents. We anticipate BrO_3^- oxidations to start off slowly and quickly gather speed as the reactive intermediates are formed autocatalytically from BrO_3^-. Trace amounts of Br^- which are normally present are sufficient to initiate the reaction:[23]

$$BrO_3^- + Br^- + 2H^+ \rightleftharpoons HBrO_2 + HOBr \quad (8)$$

HOBr can then oxidize the reductant Red, by oxygen-transfer pushing equilibrium [reaction (8)] to the right:

$$HOBr + Red \rightarrow Red - O + H^+ + Br^- \quad (9)$$

The Br^- used up in reaction (8) will be regenerated in reaction (9).

$HBrO_2$ is known to establish a rapid equilibrium in the presence of Br^-, producing more HOBr:[24]

$$HBrO_2 + Br^- + H^+ \rightleftharpoons 2HOBr \quad (10)$$

Addition of reactions (8), (9) and (10) shows that the reaction will display autocatalysis in Br^- in which 2 mol of Br^- will give 3 mol. Thus, the concentration of Br^- builds up very rapidly in the initial stages of the reaction.

Oxidation of AETSA. Recognizing that only one sulfur atom is cleaved from the parent molecule to form SO_4^{2-}, it appears that most of the oxidation activity occurs on the inner sulfur atom with subsequent cleavage of the S—S bond when the inner sulfur atom approaches oxidative saturation. The expected form of oxidation is by successive oxygen addition:

$$HOBr + RS{-}SO_3H \rightarrow RS(O)SO_3H + H^+ + Br^- \quad (11)$$

where $R = H_2NCH_2CH_2{-}$.

Timed NMR spectral scan results confirmed the postulated sulfoxide intermediate in reaction (11).

$$H_3\overset{+}{N}{-}\overset{\beta}{C}H_2{-}\overset{\alpha}{C}H_2{-}\ddot{S}{-}SO_3H$$

$$\xrightarrow{[O]} H_3N{-}CH_2{-}CH_2{-}\overset{\displaystyle O}{\overset{\|}{\ddot{S}}}{-}SO_3H \quad (11a)$$

followed by

$$H_3\overset{+}{N}{-}\overset{\beta}{C}H_2{-}\overset{\alpha}{C}H_2{-}\overset{\displaystyle O}{\overset{\|}{\ddot{S}}}{-}SO_3H$$

$$\xrightarrow{[O]} H_3\overset{+}{N}{-}\overset{\beta}{C}H_2{-}\overset{\alpha}{C}H_2{-}\overset{\displaystyle O}{\overset{\|}{\underset{\displaystyle O}{\underset{\|}{S}}}}{-}SO_3H \quad (11b)$$

After mixing acidic bromate with AETSA, NMR spectra were taken at one minute intervals. Depending upon the acid concentration (controls rate of reaction), after a short interval, it is observed that the original AETSA multiplet is spread out much further, indicating that the two sets of protons are being split by the effect of the oxygen atom attached to the inner sulfur atom. The most important feature of the NMR spectrum, however, is that two new (and transient) triplets are observed on either side of the multiplet. This can easily be explained by invoking the sulfoxide intermediate. The presence of oxygen and a lone pair on the inner sulfur atom introduces asymmetry on that sulfur atom. This asymmetry makes the two α protons diastereotopic. The two triplets represent interaction of each of the two diastereotopic hydrogens with the equivalent β protons. The addition of another oxygen atom on the middle sulfur atom to form the sulfone [see structure in reaction (11b), above] removes this diastereoisomerism and the two triplets disappear. Concurrently, with the splitting of the α, β protons, the two triplets that characterize taurine are formed. At $t = \infty$, the split peaks disappear, and one remains with the taurine triplets which, however, appear slightly downfield from those expected from standard taurine due to the formation of the mono- and di-bromotaurines.

The middle sulfur atom is the only one with two sets of lone pair electrons which lend themselves well to electrophilic attack. $RS(O)SO_3H$ can be further oxidized:

$$HOBr + RS(O)SO_3H \rightarrow RS(O)_2SO_3H + H^+ + Br^- \quad (12)$$

The next oxidation step should involve the cleavage of the S—S bond:

$$HOBr + RS(O)_2SO_3H + H_2O \rightarrow RSO_3H + SO_4^{2-} + Br^- + 3H^+ \quad (13)$$

BrO_3^- and $HBrO_2$ can also oxidize AETSA, but at much slower rates:

$$BrO_3^- + RS{-}SO_3H + H^+ \rightarrow RS(O)SO_3H + HBrO_2 \quad (14)$$

followed by

$$HBrO_2 + RS{-}SO_3H \rightarrow RS(O)SO_3H + HOBr \quad (15)$$

Reaction (14), especially, can act as the initiator of the reaction by forming $HBrO_2$ which in turn will oxidize AETSA in reaction (15) to give HOBr leading to reaction (9) which regenerates Br^-. Reaction (14) would be an initiator reaction only and would not be the rate-determining step. The kinetics data suggest that the rate-determining step is reaction (8):

$$\text{rate} = -\text{d}[\text{AETSA}]/[\text{d}t] = k_0[BrO_3^-][H^+]^2[Br^-] \quad (I)$$

Replacing Br^- with AETSA in eqn. (I) gives the maximum possible rate of reaction as the maximum amount of bromide produced, which is controlled by the amount of AETSA present [see stoichiometric eqn. (3)]. The rate of formation of Br^- is also proportional to the AETSA concentration. This is also collaborated by the data in Fig. 3 which shows a higher rate of formation of Br_2(aq) with $[AETSA]_0$.

Accumulation of Br^-. The accumulation of Br^- from the reduction of the bromine centre not only enhances the rate of formation of HOBr [reaction (10)], but it also brings into the reaction mixture a very important oxidant: Br_2(aq):[25]

$$HOBr + Br^- + H^+ \rightleftharpoons Br_2(aq) + H_2O \quad (16)$$

Br_2(aq) is a very powerful oxidizing agent and should oxidize AETSA and other intermediates by electron transfer followed by hydrolysis:

$$Br_2(aq) + RS{-}SO_3H + H_2O \rightarrow RS(O)SO_3H + 2H^+ + 2Br^- \quad (17)$$

By monitoring the reaction at the maximum absorption peak for bromine (390 nm) any accumulation of Br_2(aq) can be detected.

The question as to the significance of the appearance of Br_2 (end of induction period) can be answered by comparing the rate of the BrO_3^-–AETSA reaction with reaction (17). The BrO_3^-–AETSA reaction shows induction periods of between 20 and 300 s (depending on initial conditions), and an overall reaction time of *ca.* 5 min–24 h [for production of stoichiometric amounts of Br_2(aq)], and yet the Br_2–AETSA reaction, (17), is over in milliseconds (see Fig. 5). Thus, the presence of

Table 1 Mechanism for the oxidation of 2-aminoethanethiolsulfuric acid by bromate in acidic medium

reaction number	reaction	forward and reverse rate constants
M1	$BrO_3^- + Br^- + 2H^+ \rightleftharpoons HBrO_2 + HOBr$	2.1; 1×10^4
M2	$HBrO_2 + Br^- + H^+ \rightleftharpoons 2HOBr$	2.0×10^5; 2.0×10^{-5}
M3	$HOBr + Br^- + H^+ \rightleftharpoons Br_2 + H_2O$	8.9×10^8; 110
M4	$BrO_3^- + RS{-}SO_3H + H^+ \rightarrow RS(O)SO_3H + HBrO_2$	15.5
M5	$HOBr + RS{-}SO_3H \rightarrow RS(O)SO_3H + Br^- + H^+$	1.5×10^4
M6	$HOBr + RS(O)SO_3H \rightarrow RS(O)_2SO_3H + Br^- + H^+$	1.5×10^6
M7	$HOBr + RS(O)_2SO_3H + H_2O \rightarrow RSO_3H + SO_4^{2-} + Br^- + 3H^+$	1.0×10^3
M8	$Br_2 + RS{-}SO_3H + H_2O \rightarrow RS(O)SO_3H + 2Br^- + 2H^+$	1.0×10^8
M9	$Br_2 + RS(O)SO_3H + H_2O \rightarrow RS(O)_2SO_3H + 2Br^- + 2H^+$	8.0×10^7
M10	$Br_2 + RS(O)_2SO_3H + 2H_2O \rightarrow RSO_3H + SO_4^{2-} + 4H^+ + 2Br^-$	1.5×10^3
M11	$HOBr + RSO_3H \rightarrow BrHNR' + H_2O$	1.0×10^6
M12	$Br_2 + H_2NR' \rightarrow BrHNR' + Br^- + H^+$	5.0×10^6
M13	$2BrHNR' \rightleftharpoons H_2NR' + Br_2NR'$	110, 90

R is $H_2NCH_2CH_2-$ and R′ is $-CH_2CH_2SO_3H$

any reductant should mop up bromine from the reaction mixture. The end of the induction period thus indicates complete consumption of AETSA.

Further oxidation of taurine. NMR data shows that the taurine formed in reaction (3) is further oxidized. This oxidation can be carried out by $HOBr–OBr^-–Br_2(aq)$ to form mono- and di-bromotaurine[26]

$$HOBr + H_2NR' \rightarrow Br(H)NR' + H_2O \qquad (18)$$

(where $R' = -CH_2CH_2SO_3H$)
followed by disproportionation reaction (5) to form dibromotaurine and taurine. Proton NMR spectra of the reaction products, which show a downfield-shifted taurine spectrum, confirms that the hydrogens on the nitrogen of the amino group are replaced by more electron-withdrawing bromine atoms. The stoichiometry of the reaction before oxidation of taurine is reaction (3). Further oxidation of taurine occurs after all the AETSA has been oxidized to SO_4^{2-} and taurine.

Formation of Br_2(aq). Br_2(aq) is formed through the overall reaction represented by reaction (2) and specifically by the reaction step (16). The rate of formation of Br_2(aq) will be determined by the rates of formation of HOBr and Br^- [equilibrium (16) is rapid in both directions]. The catalysis [reactions (8) + (9) + (10)] that characterizes Br^- formation will give a sigmoidal trace for the formation of Br_2(aq).[27] In excess BrO_3^-, the amount of Br^- formed will determine the rate of formation of Br_2(aq) [from reaction (2)] as well as the amount of Br_2(aq) formed [from the stoichiometry of reaction (2)]. Higher $[AETSA]_0$ will produce more Br^- ions [reaction stoichiometry (3)]. The data shown in Fig. 3 can be explained on this basis.

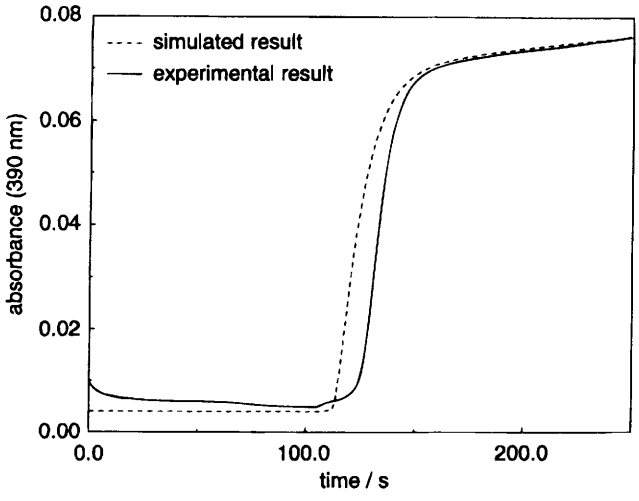

Fig. 6 Computer simulations of the Br_2(aq) formation derived from the mechanism in Table 1. The solid line represents experimental data, the dotted line represents calculated results. $[AETSA]_0 = 0.002$ M; $[H^+]_0 = 0.510$ M; $[BrO_3^-]_0 = 0.048$ M.

Computer simulations

A concise and simplified mechanism was distilled from all the possible reactions in solution. This simplified mechanism comprising of single step reactions is shown in Table 1. All sulfur–sulfur type reactions (*e.g.* dimerizations) were ignored in this mechanism. The simulations were set up for conditions of excess BrO_3^- and high acid concentrations. The overwhelming excess of oxidant, $[BrO_3^-]_0/[AETSA]_0 > 10$, discouraged the formation of dimeric or any other polymeric sulfur species. There were no kinetic experimental data available for conditions of excess $[AETSA]_0$.

There are only two types of reactions in Table 1: the standard oxyhalogen reactions (M1)–(M3) and the oxybromine–sulfur reactions, (M4)–(M12) (reactions of Br_2 are also classified under this group). The last reaction, (M13), represents the mono- and di-bromotaurine equilibrium. The mechanism, and hence the simulations was simplified by making the following assumptions: (a) oxidation by BrO_3^- is too slow to be considered, except in the initiation reaction, (M4), as well as in the rate-determining step, (M1); (b) The equilibrium in reaction (M2) is rapid enough (compared to the timescale of our overall reaction) such that HOBr can be assumed to be the sole important oxybromine oxidant. The other oxidant is Br_2(aq); (c) The oxybromine/bromine–sulfur compound reactions are essentially irreversible. Such reactions involve the reduction of the bromine centre and the oxidation of the sulfur centre. By instituting these assumptions, there were much fewer kinetics parameters to estimate and guess. The 13 equations in Table 1 were numerically integrated using a semi-implicit Runge Kutta method.[28] Kinetics parameters for the standard reactions (M1)–(M3) were taken from the literature. Kinetics parameters for reactions (M4), (M5), (M7), (M11) and (M12) were estimated from this study. Reaction (M4), in particular, was estimated by observing the initial rate of disappearance of AETSA at $\lambda = 240$ nm. At 240 nm, however, there was interference from BrO_3^- and from the dibromotaurine. The absorbance data were thus only useful within less than a minute into the reaction. Generally, rates of oxidation by Br_2(aq) and HOBr are very similar. The rate-determining reactions in our mechanism are (M1), (M4), (M7) and (M10) only. The simulations were insensitive to the rest of the parameters, as long as they were high enough not to be rate-determining.

The simulations correctly predicted the induction period (see Fig. 6) as well as the effects of acid, BrO_3^- and AETSA.

Although the model does not reproduce the kink, which marks the end of the induction period, the steep rise in absorbance at 390 nm does occur at a time close to the kink. The simulations always predicted an induction period in-between the start of the kink and the observed steep rise in absorbance.

Conclusion

The oxidation of AETSA by BrO_3^- is much simpler than the corresponding oxidation by IO_3^-. The rapid Br_2(aq)–AETSA reaction precludes the possibility of oligo-oscillations.[29] The large difference in reaction rates of the BrO_3^-–AETSA and Br_2–AETSA systems is not conducive to the effective coupling necessary for oligo-oscillatory behaviour.[30] The only complexity yet unexplained is the 'kink' observed after the end of the induction period. This can be rationalized by observing that the depletion of AETSA allows reaction (16) to start producing Br_2(aq) and signal the end of the induction period. The commencement of reaction (4), however brings out a temporary depletion of Br_2(aq). This is very short-lived [consumption of Br_2(aq)] as reaction (4) produces Br^- which will produce more HOBr [reaction (9)] and subsequently more Br_2(aq) [reaction (17)].

We would like to thank the University of the North (Sovenga, South Africa) for giving leave of absence to one of us (J.D.). This work was initially sponsored by an NSF-EPSCoR grant to the West Virginia University Non-linear Dynamics Cluster. In the final stages the work was sponsored by NSF Grant Number 9632592.

References

1 R. H. Simoyi, M. Manyonda, J. Masere, M. Mtambo, I. Ncube, H. Patel, I. R. Epstein and K. Kustin, *J. Phys. Chem.*, 1991, **95**, 770.
2 R. C. Thompson, *Inorg. Chem.*, 1973, **8**, 1905.
3 R. H. Simoyi, *J. Phys. Chem.*, 1985, **89**, 3570.
4 I. R. Epstein, *The Search for New Chemical Oscillators*, in *Chemical Instabilities*, ed. G. Nicolis, D. Reidel, Dordrecht, Holland, 1984, vol. 3.
5 B. P. Belousov, *Sb. Ref. Radiat. Med.*, Medgdiz, Moscow, 1958, **145**, 1959.
6 R. J. Field, E. Koros and R.M. Noyes, *J. Am. Chem. Soc.*, 1972, **94**, 8649.
7 R. H. Simoyi and R. M. Noyes, *J. Phys. Chem.*, 1987, **91**, 2689.
8 P. De Kepper, I. R. Epstein and K. Kustin, *J. Am. Chem. Soc.*, 1981, **103**, 2133.
9 Y. Luo, M. Orban, K. Kustin and I. R. Epstein, *J. Am. Chem. Soc.*, 1989, **111**, 4541.
10 M. Orban and I. R. Epstein, *J. Am. Chem. Soc.*, 1985, **107**, 2302.
11 I. Nagypal, I. R. Epstein and K. Kustin, *Int. J. Chem. Kinet.*, 1986, **18**, 345.
12 R. H. Simoyi, J. Masere, C. Muzimbaranda, M. Manyonda and S. Dube, *Int. J. Chem. Kinet.*, 1991, **23**, 419.
13 R. H. Simoyi and I. R. Epstein, *J. Phys. Chem.*, 1987, **91**, 5124.
14 R. H. Simoyi, I. R. Epstein and K. Kustin, *J. Phys. Chem.*, 1989, **93**, 2792.
15 E. Mambo and R. H. Simoyi, *J. Phys. Chem.*, 1993, **97**, 13662.
16 C. R. Chinake and R. H. Simoyi, *J. Phys. Chem.*, 1993, **97**, 11569.
17 C. Mundoma and R. H. Simoyi, *J. Chem. Soc., Faraday Trans.*, submitted.
18 S. J. Dushman, *J. Phys. Chem.*, 1904, **8**, 453.
19 D. A. Skoog and D. M. West, *Analytical Chemistry: An Introduction*, Saunders Golden Publishing, Philadelphia, 1985, p. 323.
20 Y. Y. Lin, C. E. Wright, M. Zagorski and K. Nakanishi, *Biochim. Biophys. Acta*, 1988, **969**, 242.
21 D. C. Harris, *Quantitative Chemical Analysis*, W. H. Freeman and Company, San Francisco, 1982, p. 384.
22 E. L. Thomas, P. M. Bozeman, M. M. Jefferson and C. C. King, *J. Biol. Chem.*, 1995, **270**, 2906.
23 C. R. Chinake, R. H. Simoyi and S. B. Jonnalagadda, *J. Phys. Chem.*, 1994, **98**, 545.
24 K. Bar-Eli, *J. Phys. Chem.*, 1985, **89**, 2855.
25 M. Eigen and K. Kustin, *J. Am. Chem. Soc.*, 1962, **84**, 1355.
26 J. M. Antelo, F. Arce, M. C. Castro, J. Crugeiras, J. C. Perez-Moure and P. Rodriguez, *Int. J. Chem. Kinet.*, 1995, **27**, 703
27 J. I. Steinfeld, J. S. Francisco and W. I. Hase, *Chemical Kinetics and Dynamics*, Prentice Hall, Englewood Cliffs, 1989, p. 182.
28 P. Kaps and P. Rentrop, *Numer. Math.*, 1979, **23**, 55.
29 C. R. Chinake, E. Mambo and R. H. Simoyi, *J. Phys. Chem.*, 1994, **98**, 2908.
30 G. Y. Rabai and M. T. Beck, *J. Chem. Soc., Dalton Trans.*, 1985, 1669.

Paper 6/02856J; *Received* 23*rd April*, 1996